

# Pathogenic Role for Virus-Specific CD4 T Cells in Mice with Coronavirus-Induced Acute Encephalitis

Daniela Anghelina,\* Lecia Pewe,<sup>†</sup> and Stanley Perlman\*<sup>†‡</sup>

From the Interdisciplinary Program in Neuroscience\* and Departments of Pediatrics<sup>†</sup> and Microbiology,<sup>‡</sup> University of Iowa, Iowa City, Iowa

**Acute viral encephalitis is believed to result from direct virus destruction of infected cells and from virus-induced host immune response, but the relative contribution of each remains largely unknown. For example, C57BL/6 (B6) mice infected with mouse hepatitis virus (JHM strain, JHMV) develop severe encephalitis, with death occurring within 7 days. Here, we show that the host response to a single JHMV-specific immunodominant CD4 T-cell epitope is critical for severe disease. We engineered a recombinant JHMV with mutations in the immunodominant CD4 T-cell epitope (rJ.M<sub>Y135Q</sub>). Infection of naïve B6 mice with this virus resulted in mild disease with no mortality. However, introduction of a CD4 T-cell epitope from *Listeria monocytogenes* into rJ.M<sub>Y135Q</sub> generated a highly virulent virus. The decrease in disease severity was not due to a switch from Th1 to Th2 predominance in rJ.M<sub>Y135Q</sub>-infected mice, an effect on CD8 T-cell function, or differential expression of tumor necrosis factor- $\alpha$  by JHMV-specific CD4 T cells. These results show that the response to a single virus-specific CD4 T-cell epitope may contribute to a pathogenic host response in the setting of acute viral disease and that abrogation of this response ameliorates clinical disease without diminishing virus clearance. (*Am J Pathol* 2006, 169:209–222; DOI: 10.2353/ajpath.2006.051308)**

Mice infected with the JHM strain of mouse hepatitis virus (JHMV), a neurotropic coronavirus, develop acute and chronic diseases of the central nervous system. The JHMV-infected mouse is most often studied as a model of chronic demyelination because it has similarities to the disease observed in humans with multiple sclerosis.<sup>1,2</sup> Myelin destruction in these animals occurs as a direct consequence of virus clearance and is largely immune-

mediated because it does not occur to a significant extent in mice lacking T or B cells (lethally irradiated mice, mice with severe combined immunodeficiency, or mice lacking recombination activation enzyme gene 1 [RAG1<sup>-/-</sup>]).

Less is known about the role of the adaptive immune response in JHMV-mediated acute encephalitis. After intranasal inoculation, virus spreads from the olfactory bulb transneuronally to its primary, secondary, and tertiary connections. By day 7 post inoculation (p.i.), virus is partly cleared from the front of the brain but is present at high levels in more distal regions such as the medial parabrachial nucleus and brainstem reticular formation. Most notably, JHMV only rarely infects the CA1 and CA3 regions of the hippocampus, unlike other viruses that cause acute encephalitis, such as HSV-1.<sup>3,4</sup> Clinical signs of disease first become apparent at approximately 5 days p.i., and mice are moribund by 7 to 8 days p.i.<sup>3,5</sup> Neutrophils, macrophages, and NK cells are detected as early as day 3 p.i. with T-cell infiltration first noted at day 5 p.i.<sup>6,7</sup> The innate immune response may be important in the development of disease; consistent with this, evidence of cytokine and chemokine dysregulation in mice with JHMV-induced fatal acute encephalitis has been reported.<sup>8</sup> However, other observations are consistent with a role for the T-cell response in the development of clinical disease. Thus, although high titers of infectious virus are detected in mice dying from acute encephalitis, titers decline slightly from days 5 to 7 p.i. as mice deteriorate clinically and virus is cleared from ventral portions of the brain.<sup>5,8,9</sup> JHMV-specific CD4 and CD8 T cells are not detected in appreciable numbers until day 6 p.i., 1 to 2 days before the death of the animals and concomitant with the onset of virus clearance.<sup>7</sup> These studies raised the possibility that virus-specific T cells, although required for virus clearance,<sup>2,10</sup> are critical for the development of severe clinical disease in mice with acute encephalitis.

Supported in part by grants from the National Institutes of Health (NS36592) and the National Multiple Sclerosis Society (RG2864).

Accepted for publication April 4, 2006.

Address reprint requests to Dr. Stanley Perlman, Department of Pediatrics, University of Iowa, Medical Laboratories 2042, Iowa City, IA 52242. E-mail: stanley-perlman@uiowa.edu.

Observations from other models of JHMV-mediated disease also suggest a role for T cells in enhanced clinical disease, independent of any role that these cells have in demyelination. For example, *RAG1*<sup>-/-</sup> mice infected with an attenuated strain of JHMV generally remain asymptomatic until approximately 14 to 18 days p.i., at which point they develop signs of fatal encephalitis. However, adoptive transfer of total splenocytes from JHMV-immune mice at 4 days p.i., which results in partial virus clearance and the development of clinical disease (hindlimb paresis and mild encephalitis), shortens the asymptomatic period to 11 days p.i. The development of clinical disease is accelerated further if CD4 T-cell-enriched splenocytes are transferred, with clinical signs of severe encephalitis detected as early as 9 to 10 days p.i. and death occurring over the subsequent 24 to 48 hours.<sup>11-13</sup>

At least three CD4 T-cell epitopes are recognized in C57BL/6 (B6) mice infected with JHMV, with a large fraction of the response (up to 25%) directed against an epitope encompassing residues 133 to 147 of the transmembrane (M) protein (epitope M133).<sup>7,14</sup> It is well established that virus clearance is delayed in many viral central nervous system (CNS) infections if the CD4 T-cell response is completely abrogated, with a consequence of more severe disease.<sup>15-19</sup> Therefore, to probe the potentially pathogenic role of CD4 T cells in JHMV-mediated acute encephalitis, we used reverse genetics to engineer a virus with mutations in the immunodominant epitope M133. CD4 T cells in mice infected with this virus still recognize subdominant JHMV-specific CD4 T-cell epitopes. Our results show that elimination of the CD4 T-cell response to this single epitope resulted in a reduction in mortality from 100 to 0%.

## Materials and Methods

### Mice

Specific pathogen-free 5- to 6-week-old B6 and BALB/c mice (National Cancer Institute, Bethesda, MD) and *RAG1*<sup>-/-</sup> mice (Jackson Laboratories, Bar Harbor, ME) were inoculated intranasally (i.n.) with 4 to 8 × 10<sup>4</sup> plaque forming units of virus in 12 μl of Dulbecco's modified Eagle's medium. Mice were examined and weighed daily. In all experiments, surviving mice were euthanized at 16 days p.i. Virus was harvested from the infected CNS and titered by plaque assay on HeLa cells expressing the cellular receptor for mouse hepatitis virus, CEACAM1 (HeLa-MHVR). In some experiments, B6 mice were inoculated with 3 to 5 × 10<sup>6</sup> colony forming units of attenuated recombinant actA-deficient strain of *Listeria monocytogenes* 1 month before infection with virus. These *L. monocytogenes* (LM)-immune mice were kindly provided by Dr. J. Haring, University of Iowa. All animal studies were approved by the University of Iowa Animal Care and Use Committee.

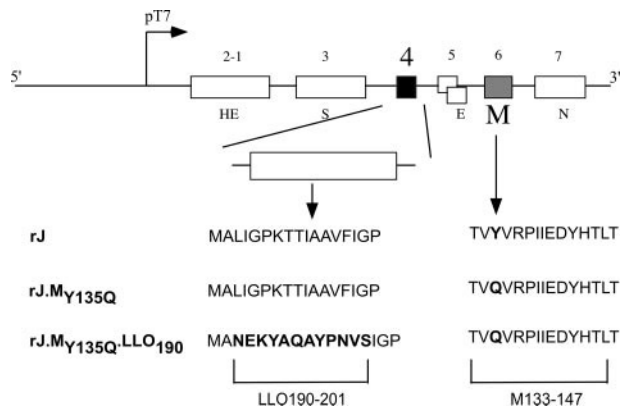


**Figure 1.** Schematic diagram of recombinant JHMV constructs. Recombinant rJ, rJ.MY135Q, and rJ.MY135Q.LLO190 were engineered as described in Materials and Methods. A mutation to abrogate recognition by epitope M133-specific CD4 T cells (Y135Q) was introduced into the M gene in rJ.MY135Q. The LLO190 epitope from LM was introduced into gene 4 of rJ.MY135Q to generate rJ.MY135Q.LLO190.

### Viruses and Cells

JHMV was grown and titered as described previously.<sup>20</sup> A chimeric recombinant virus encoding the feline S protein (designated fMHV-JHM clone B4c) was used as a recipient for targeted recombination.<sup>21,22</sup> All recombinant viruses encoding the MHV S protein were propagated in mouse 17Cl-1 cells and titered on HeLa-MHVR cells.

### Recombinant Viruses

Recombinant viruses were generated by targeted recombination as described previously.<sup>21,22</sup> In brief, a plasmid containing genes 2 to 7 of JHM.IA<sup>21</sup> was used as the substrate for RNA synthesis. We used overlapping extension polymerase chain reaction (PCR) to mutate epitope M133 (Tyr to Gln at position 135; pJ.MY135Q). The two inner primers used were 5'-GTACCGTGCAAGTTAGACC-3' (forward) and 5'-GGGTCTAACTTGCACGGTAC-3' (reverse) (mutations responsible for Tyr to Gln change at amino acid M135 are underlined). The outer primers were 5'-CTACCAATGGACGGCCGACGAGG-3' (forward; nucleotides 29,174 to 29,196) and 5'-CCAGATCGGCTAGCAGGTGCAGACC-3' (reverse; nucleotides 30,429 to 30,453). The overlapping PCR product was subcloned into pCR2.1-TOPO (pCR2.1.MY135Q). A DNA fragment was excised from pCR2.1.MY135Q with *MfeI* and *NheI* and inserted into pJHM.IA. Donor RNAs were transcribed using T7 polymerase and transfected into feline cells (AK-D) previously infected with fMHV-JHM (a recombinant MHV strain encoding the feline surface (S) glycoprotein). fMHV-JHM does not infect murine cells, but recombinant virus expressing the MHV S protein does, allowing for efficient selection of recombinant virus on 17Cl-1 murine cells. Recombinant virus rJ.MY135Q was propagated as previously described (Figure 1).<sup>21</sup>

A second set of recombinants was also engineered in which a CD4 T-cell epitope from LM-encompassing residues 190 to 201 of listeriolysin O (epitope LLO190, NEKYAQAYPNVS<sup>23</sup>) was inserted into gene 4 of rJ.MY135Q by overlapping extension PCR, resulting in

rJ.M<sub>Y135Q</sub>.LLO<sub>190</sub>. We showed previously that insertions into gene 4 did not affect virus growth in tissue culture or the ability to cause acute encephalitis.<sup>21</sup> Outer primers were 5'-CCAAGCAATTCAGTGATAGTAGTACGC-3' (forward) and 5'-CCTCTTGAACACCAAG-3' (reverse). Inner primers were 5'-GCTCAAGCTTATCCAAATGTAAG-TATTGGTCCATTCTAGTAGCA-3' (forward) and 5'-GCTTGAGCATATTTTCATTGGCCATAACTACTTGGCTGC-C-3' (reverse) (LLO190 epitope is underlined). PCR products were prepared, subcloned, and eventually inserted into pJ.M<sub>Y135Q</sub> (pJ.M<sub>Y135Q</sub>.LLO<sub>190</sub>) (Figure 1). Recombinant virus was isolated as described above. In all cases, viruses were sequenced to confirm the presence of the introduced mutations before inoculation into mice. To control for any unwanted mutations that might have occurred during the process of targeted recombination, at least two independent isolates of each recombinant virus were analyzed in these studies.

### RNA Sequence Analysis

Mice were infected with virus intranasally. At day 7, mice were sacrificed, and RNA was harvested from one-half of each brain as described previously.<sup>24</sup> To confirm that no changes occurred in epitopes M133<sub>Y135Q</sub> or LLO190 during passage in mice, cDNA was prepared, and PCR products encompassing the two epitopes were sequenced.

### Growth Kinetics in Tissue Culture Cells

Confluent 17Cl-1 monolayers in 12-well plates were infected with viruses at a multiplicity of infection of 1, as described previously.<sup>21</sup> Samples were harvested at the times indicated, and viral titers were determined on HeLa-MHVR cells. In all experiments in which virus titers were measured, cells and supernatants were combined before determining titer.

### pH and Thermal Inactivation

Equal amounts of rJ and rJ.M<sub>Y135Q</sub> were diluted in Dulbecco's modified Eagle's medium buffered to pH 6.0, 7.0, or 8.0, prepared as previously described.<sup>25</sup> Viruses were incubated at 37°C for the indicated times and subsequently titered on HeLa-MHVR cells.

### Intracellular Cytokine Staining

Cells were prepared from infected brains and analyzed for cytokine production after stimulation with JHMV-specific peptides as previously described.<sup>12</sup> Peptides corresponding to the immunodominant CD8 T-cell epitope recognized in B6 mice (epitope S510) or irrelevant peptide (Ova 257–264) were used at a final concentration of 1 μmol/L. Peptides corresponding to the CD4 T-cell epitopes M133, M133<sub>Y135Q</sub>, LLO190, S333, and S358 were used at a final concentration of 5 μmol/L, except for peptide LLO190, which was used at 8 μmol/L. Briefly,

cells were washed, permeabilized, and incubated in blocking buffer containing 10% rat serum and anti-FcγRIII/II Ab (2.4G2). Cells were then stained with fluorescein isothiocyanate (FITC) anti-mouse CD8α monoclonal antibody (mAb) (Ly-2, clone 53–6.7) or FITC anti-mouse CD4 mAb (L3T4, clone GK1.5), respectively. Cells were stained for intracellular IFN-γ or tumor necrosis factor-α (TNF-α) using phycoerythrin-conjugated anti-IFN-γ or allophycocyanin-conjugated anti-TNF-α, respectively. All reagents were purchased from BD Pharmingen (San Diego, CA). After washing and fixation, cells were analyzed using a FACScan Flow Cytometer (BD Biosciences, Mountain View, CA). The number of lymphocytes harvested from each infected brain ranged from 1 × 10<sup>6</sup> to 3 × 10<sup>6</sup>.

### Macrophage/Microglia and Neutrophil Enumeration

Cells were prepared from infected brains and incubated in blocking buffer containing 10% rat serum and anti-FcγRIII/II Ab (2.4G2). Cells were then stained with PerCP-conjugated rat anti-CD45 (mAb 30-F11; BD Pharmingen), rat PE-conjugated rat anti-F4/80 (macrophages/microglia, cl BM-8; Caltag Laboratories, Burlingame, CA), and FITC-conjugated anti-Ly6G (neutrophils, mAb 1A8; BD Pharmingen) and then analyzed using a FACScan Flow Cytometer. Macrophages/microglia were identified as CD45<sup>hi/int</sup>F4/80<sup>+</sup>Ly6G<sup>-</sup>, whereas neutrophils were CD45<sup>hi</sup>F4/80<sup>-</sup>Ly6G<sup>+</sup>.

### Virus Antigen Detection

For immunohistochemistry, brain and spinal cord sections were fixed in zinc formalin and processed as previously described.<sup>11</sup> Sections were probed with antibody directed against the JHMV nucleocapsid (N) protein (mAb 5B188.2, 1:10,000; kindly provided by Dr. M. Buchmeier [The Scripps Research Institute, La Jolla, CA]) followed by biotinylated goat anti-mouse (1:100; Jackson Immunoresearch, West Grove, PA). Sections were developed by sequential incubation with streptavidin-horseradish peroxidase conjugate and diaminobenzidine (Sigma, St. Louis, MO).

### Staining with Tetramers

Cells were harvested from the CNS of infected mice and stained with MHC class I/S510 (CSLWNGPHL) tetrameric complexes, obtained from the National Institutes of Health Tetramer Core Facility, Atlanta, GA, as described previously.<sup>26</sup>

### Cytotoxic T-Cell Assays

Mononuclear cells were harvested from the brains of B6 mice infected with rJ or rJ.M135Q and analyzed in direct *ex vivo* chromium release cytotoxicity assays as previously described.<sup>27</sup> Target cells were EL-4 cells coated

with peptide at a final concentration of 1  $\mu\text{mol/L}$  or left uncoated. The percent specific release was defined as  $100 \times (\text{experimental release} - \text{spontaneous release}) / (\text{total release} [\text{detergent-treated}] - \text{spontaneous release})$ . Maximum spontaneous release was  $<10\%$  in all experiments.

### Interleukin (IL)-5 Enzyme-Linked Immunospot (ELISPOT) Assay

IL-5 ELISPOT assays were performed as described previously.<sup>28</sup> Briefly, nitrocellulose-based 96-well plates (Millititer HA, Millipore, Bedford, MA) were coated overnight at 4°C with 5  $\mu\text{g/ml}$  anti-IL-5 (clone TRFK5; eBioscience, San Diego, CA), 2.5  $\mu\text{g/ml}$  anti-CD3 (clone 145-2C11; eBioscience), and 2.5  $\mu\text{g/ml}$  anti-CD28 mAb (clone 37-51; eBioscience) diluted in phosphate-buffered saline (PBS), washed the next day with PBS, and blocked with RPMI-10% fetal calf serum. After washing with PBS, CNS-derived lymphocytes from two rJ-infected mice and five rJ.M<sub>Y135Q</sub> mice were added to the wells in triplicate ( $10^5$  to  $2 \times 10^5$  cells/well), in a total volume of 200  $\mu\text{l/well}$ . Plates were incubated at 37°C for 48 hours and washed with PBS-0.05% Tween 20 (Sigma), followed by sequential incubation with biotinylated anti-IL-5 (clone TRFK4; eBioscience) and avidin-peroxidase (1/400 dilution; Sigma). Spots were visualized using 3-amino-9-ethylcarbazole (Sigma). Plates were analyzed using an immunospot analyzer (Cellular Technology Laboratory, Cleveland, OH) according to the manufacturer's instructions. The number of spots per  $1 \times 10^4$  CD4 T cells was calculated from the frequency of CD4<sup>+</sup> cells as determined by fluorescence activated cell sorting (FACS).

### Real-Time Reverse Transcriptase (RT)-PCR

Total RNA was isolated from brains using Tri Reagent (Molecular Research Center, Cincinnati, OH) following the manufacturer's instructions. cDNA was prepared as previously described<sup>24</sup> and was subjected to PCR as follows. Two microliters of cDNA was added to a 23- $\mu\text{l}$  PCR cocktail containing 2 $\times$  SYBR Green Master Mix (Applied Biosystems, Foster City, CA) and 0.2  $\mu\text{mol/L}$  each of sense and antisense primers (Integrated DNA Technologies, Coralville, IA). Amplification was then performed in an Applied Biosystems Prism 7700 thermocycler. Specificity of the amplification was confirmed using melting curve analysis. Data were collected and recorded by the Prism 7700 software and expressed as a function of threshold cycle. Specific primer sets used for TNF- $\alpha$  and a murine housekeeping gene were as follows: TNF- $\alpha$  forward, 5'-GCCTCTTCTCATTCTGCTT-3'; TNF- $\alpha$  reverse, 5'-GGTGGTTTGCTAGCACGTG-3'; HPRT forward, 5'-CCTCATGGACTGATTATGGAC-3'; HPRT reverse, 5'-CAGATCAACTGCGCTCATC-3'. TNF- $\alpha$  RNA abundance was calculated using methods described previously.<sup>29</sup>

### Statistics

A two-tailed unpaired Student's *t*-test was used to analyze differences in mean values between groups. All results are expressed as means  $\pm$  SEM. *P* values of  $<0.05$  were considered statistically significant.

### Results

#### The Y135Q Mutation in M Protein Abrogated Recognition by CD4 T Cells

Recent advances in coronavirus reverse genetics make it possible to introduce mutations into the JHMV genome.<sup>30,31</sup> We used one of these methods, targeted recombination,<sup>30</sup> to introduce a mutation into epitope M133, the immunodominant CD4 T-cell epitope recognized in B6 mice. Using a previously described motif for peptides binding to the I-A<sup>b</sup> molecule,<sup>32</sup> we identified a tyrosine at position 135 of the M protein as a likely anchor residue for binding to the MHC class II molecule. In preliminary experiments, we showed that a peptide containing the Y135Q change was no longer recognized by CD4 T cells harvested from the CNS of mice acutely infected with JHMV. This mutation was introduced into JHMV to create a recombinant virus, rJ.M<sub>Y135Q</sub>, as described in Materials and Methods and Figure 1. Two independent isolates were identified, and the presence of the mutation was confirmed by sequence analysis after amplification in tissue culture cells. To confirm the loss of recognition of the epitope in the context of infectious virus, lymphocytes were harvested from the CNS of mice inoculated with wild-type recombinant virus (rJ) or rJ.M<sub>Y135Q</sub> and analyzed for interferon- $\gamma$  (IFN- $\gamma$ ) production after stimulation with peptide M133 (Figures 2, A and B; Table 1). As expected, rJ but not rJ.M<sub>Y135Q</sub> elicited an epitope M133-specific CD4 T-cell response. Furthermore, mice infected with rJ.M<sub>Y135Q</sub> did not mount a *de novo* CD4 T-cell response to the variant M133 epitope (Figure 2B, right panel).

#### The Y135Q Mutation Did Not Affect Virus Growth in Tissue Culture Cells but Had a Modest Effect on Virus Thermostability

Epitope M133 is located in the M protein, which is required for virus assembly. The M protein interacts with both the envelope (E) and spike (S) proteins<sup>33</sup> and is therefore likely not to have a high tolerance for structural changes. Therefore, before analyzing this virus in infected mice, we assessed whether the mutation at position 135 affected growth in tissue culture cells. On infection of 17C1-1 cells, rJ and rJ.M<sub>Y135Q</sub> exhibited similar kinetics of growth, showing that the mutation in the M protein did not affect the ability of the virus to replicate and assemble *in vitro* (Figure 3A).

A sensitive assay for measuring virus stability involves determining the kinetics of virus inactivation at different pHs and temperatures.<sup>25,34</sup> For this purpose, we mea-

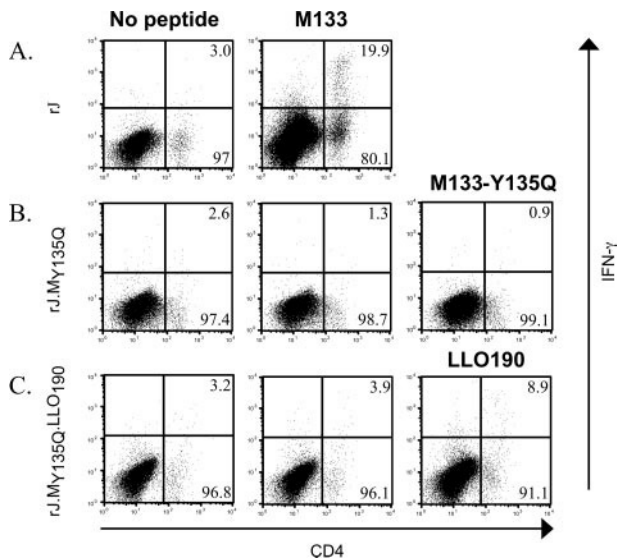


**Figure 2.** Detection of epitope M133- and LLO190-specific CD4 T cells in the CNS of infected mice. Cells were harvested from the brains of 5- to 6-week-old B6 mice 7 days after i.n. infection with rJ (A), rJ.M<sub>Y135Q</sub> (B), or rJ.M<sub>Y135Q</sub>.LLO<sub>190</sub> (C). JHMV-specific CD4 T cells were identified by intracellular staining for IFN- $\gamma$  after stimulation with cognate peptides and FACS analysis as described in Materials and Methods. Individual mice were analyzed in these assays. The percentage of IFN- $\gamma^+$  and IFN- $\gamma^-$  CD4 T cells is shown. Note that the Y135Q mutation in the M protein abrogated recognition by epitope M133-specific CD4 T cells and variant peptide M133-Y135Q did not elicit a *de novo* CD4 T-cell response (B, right panel). The CD4 T-cell response was analyzed in 6 to 12 experiments.

sured the kinetics of rJ and rJ.M<sub>Y135Q</sub> survival at 37°C at three different pHs (6, 7, and 8) (Figure 3B). The effect of the M<sub>Y135Q</sub> mutation was fairly subtle. Both viruses exhibited similar stability at pH 7, but rJ was modestly more stable at pH 6. On the other hand, rJ.M<sub>Y135Q</sub> was more stable at pH 8.

### rJ.M<sub>Y135Q</sub>: Unlike rJ, Did Not Cause Lethal Encephalitis in B6 Mice

To determine the role of the epitope M133-specific CD4 T-cell response in acute disease, 5-week-old B6 mice were infected intranasally with rJ or rJ.M<sub>Y135Q</sub>. In agreement with previous results,<sup>21</sup> all mice infected with rJ developed encephalitis and died at days 6 to 8 p.i. By contrast, mice infected with rJ.M<sub>Y135Q</sub> developed signs of mild disease, with transient hunching. No mice inoculated with rJ.M<sub>Y135Q</sub> died, and mice were completely asymptomatic when sacrificed at day 16 p.i. (Figure 4A). Mice infected with rJ showed significant weight loss, whereas, consistent with the clin-

ical signs, rJ.M<sub>Y135Q</sub>-infected mice did not lose weight (Figure 4B). These differences in clinical disease could not be attributed to varying virus loads because titers in the CNS of mice infected with rJ and rJ.M<sub>Y135Q</sub> were indistinguishable when analyzed at days 3 to 7 p.i. (Figure 4C). By day 12 p.i., virus was cleared from some rJ.M<sub>Y135Q</sub>-infected mice and present at low levels in the remainder. Virus was cleared from all mice by day 16 p.i. Furthermore, the brains of mice infected with rJ or rJ.M<sub>Y135Q</sub> all showed evidence of severe encephalitis, with widespread parenchymal and perivascular inflammatory cell infiltration detected at day 7 p.i. (Figure 5, A and B). To begin to quantify the inflammatory response, we measured the numbers of CD4 and CD8 T cells, macrophages/microglia, and neutrophils in the brains of mice infected with rJ or rJ.M<sub>Y135Q</sub> at 5 or 7 days p.i. (Figure 5, E and F). CD4 T cells facilitate optimal macrophage infiltration into the CNS, and both macrophages and neutrophils contribute to enhanced disease in the CNS.<sup>13,35,36</sup> However, similar numbers of T cells, macrophages, and neutrophils were present in the CNS of mice infected with either virus, demonstrating that the absence of an immune response to epitope M133 did not impair infiltration of these cells into the CNS. Another possible explanation for our results was that rJ and rJ.M<sub>Y135Q</sub> spread to different anatomical sites in the brain after intranasal inoculation, resulting in differences in clinical disease. However, we observed that rJ and rJ.M<sub>Y135Q</sub> spread to the same regions of the CNS (eg, olfactory bulb and tract, primary olfactory cortex, basal forebrain, lateral hypothalamus, and brainstem reticular formation<sup>3</sup>) and similar numbers of cells were infected within each of these regions, as assessed by immunohistochemical detection of virus antigen (Figure 5, C and D).

We performed additional assays to show that the difference in clinical disease was due to the loss of the epitope M133-specific CD4 T-cell response and not to a nonspecific effect on M protein function. If the absence of the CD4 T-cell response to this immunodominant epitope was critical, restoration of epitope M133 or an equivalent one should result in a virus with increased pathogenicity. For this purpose, another set of recombinant viruses was engineered, in which the I-A<sup>P</sup>-restricted CD4 T-cell epitope from *L. monocytogenes* was introduced into gene 4 (rJ.M<sub>Y135Q</sub>.LLO<sub>190</sub>), as described in Materials and Methods and Figure 1. Exogenous genetic information is commonly engineered into gene 4 because abrogation of gene 4 expression does not diminish neurovirulence in

**Table 1.** Antigen Specificity of CD4 T Lymphocytes Harvested from CNS of Mice at Day 7 p.i.

Virus	No. of mice	% CD4	M133*		LLO190*		S333*		S358*	
			%	n ( $\times 10^4$ )	%	n ( $\times 10^3$ )	%	n ( $\times 10^3$ )	%	n ( $\times 10^3$ )
rJ	6	2.8 $\pm$ 0.5	21.2 $\pm$ 1.2	1.6 $\pm$ 0.3	N.D.	N.D.	2.4 $\pm$ 0.1	2.0 $\pm$ 0.2	10.2 $\pm$ 0.9	7.5 $\pm$ 1.5
rJ.M <sub>Y135Q</sub>	12	2.3 $\pm$ 0.2	0	0	N.D.	N.D.	3.1 $\pm$ 0.5	1.6 $\pm$ 0.4	6.8 $\pm$ 1.2	3.3 $\pm$ 0.7
rJ.M <sub>Y135Q</sub> .LLO <sub>190</sub>	11	3.6 $\pm$ 0.3	0	0	4.3 $\pm$ 0.8	3.3 $\pm$ 0.7	2.1 $\pm$ 0.4	1.7 $\pm$ 0.4	8.0 $\pm$ 0.7	5.7 $\pm$ 0.8

\*No. and percentage of virus-specific CD4 T cells after subtracting background (no peptide). N.D., not determined.

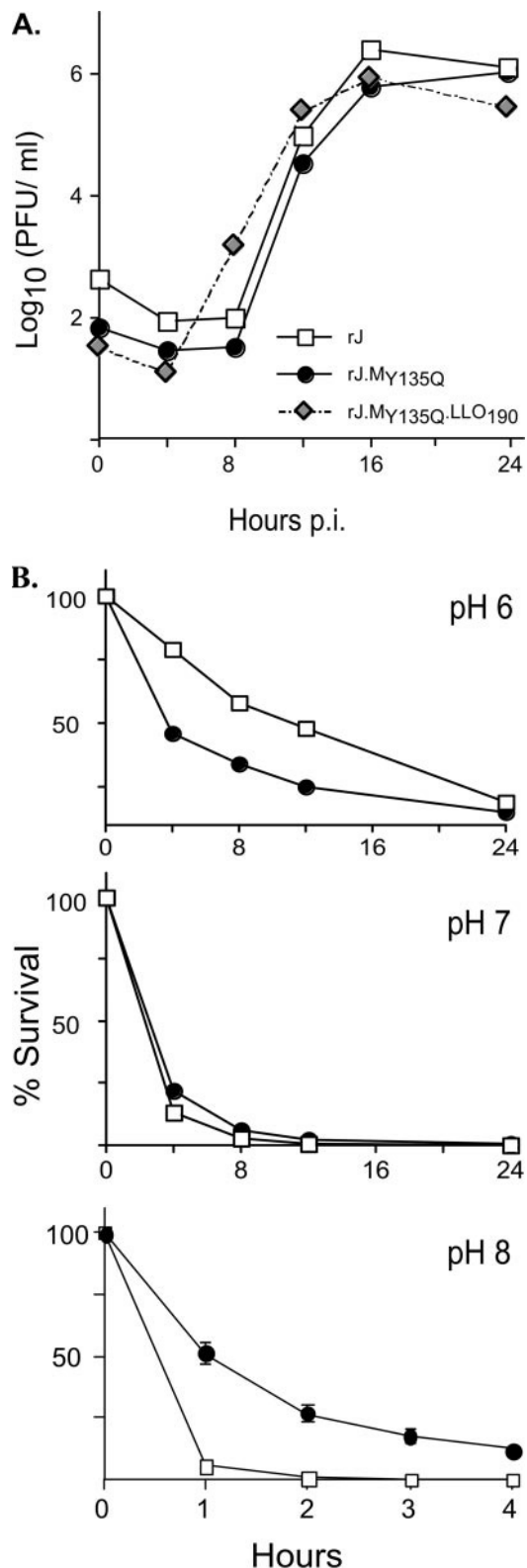


**Figure 3.** Kinetics of virus production in 17Cl-1 cells and thermal stability of recombinant viruses. **A:** 17Cl-1 cells were infected with recombinant viruses at 1 plaque forming unit/cell. Cells and supernatant were harvested at the indicated times, and titers were measured by plaque assay on HeLa-MHVR cells. Each virus was assayed in two to three independent experiments. **B:** Cell-free virus was incubated in solutions at a pH of 6, 7, or 8 at 37°C. Aliquots were removed at the indicated time points and titered on HeLa-MHVR cells. The fraction of virus surviving at each time point is shown. Data are representative of three independent experiments.

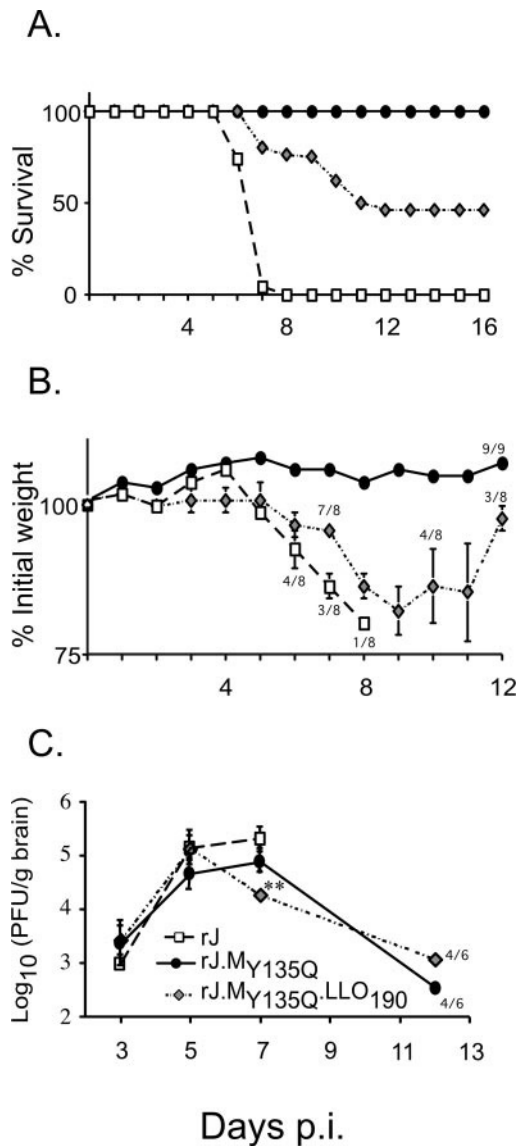


**Figure 4.** Mortality, weight loss, and virus titers in B6 mice infected with recombinant viruses. **A:** B6 mice were infected with rJ ( $n = 23$ ), rJ.MY135Q ( $n = 23$ ), or rJ.MY135Q.LLO190 ( $n = 23$ ) and monitored for survival. **B:** Eight rJ-, eight rJ.MY135Q.LLO190-, and nine rJ.MY135Q-infected mice were weighed daily. Weights relative to weight at onset of experiment are shown for mice surviving at each time point. **C:** A total of 87 B6 mice were used for determining CNS virus titers with six to nine mice assayed at the indicated time points for each virus. Significant decreases in virus titers were detected in the CNS of rJ.MY135Q.LLO190-infected mice at day 7, when compared with mice infected with rJ or rJ.MY135Q (\*\* $P < 0.005$ ). At day 12, virus was cleared from two of six mice infected with rJ.MY135Q or rJ.MY135Q.LLO190; average titers are shown for those mice with detectable virus.

mice.<sup>21</sup> As expected, mice infected with this virus mounted a CD4 T-cell response to epitope LLO190 but not to epitope M133 (Figure 2C; Table 1). Next, we infected a group of B6 mice with this virus, in parallel with rJ and rJ.MY135Q. As shown in Figure 4A, approximately 50% of the rJ.MY135Q.LLO190-infected mice died within 12 days p.i., and mice infected with this virus exhibited weight loss (Figure 4B). Virus titers were similar to those observed in mice infected with rJ or rJ.MY135Q, although they were significantly lower at day 7 p.i. ( $P < 0.005$ ) (Figure 4C). Thus, the CD4 T-cell response to epitope

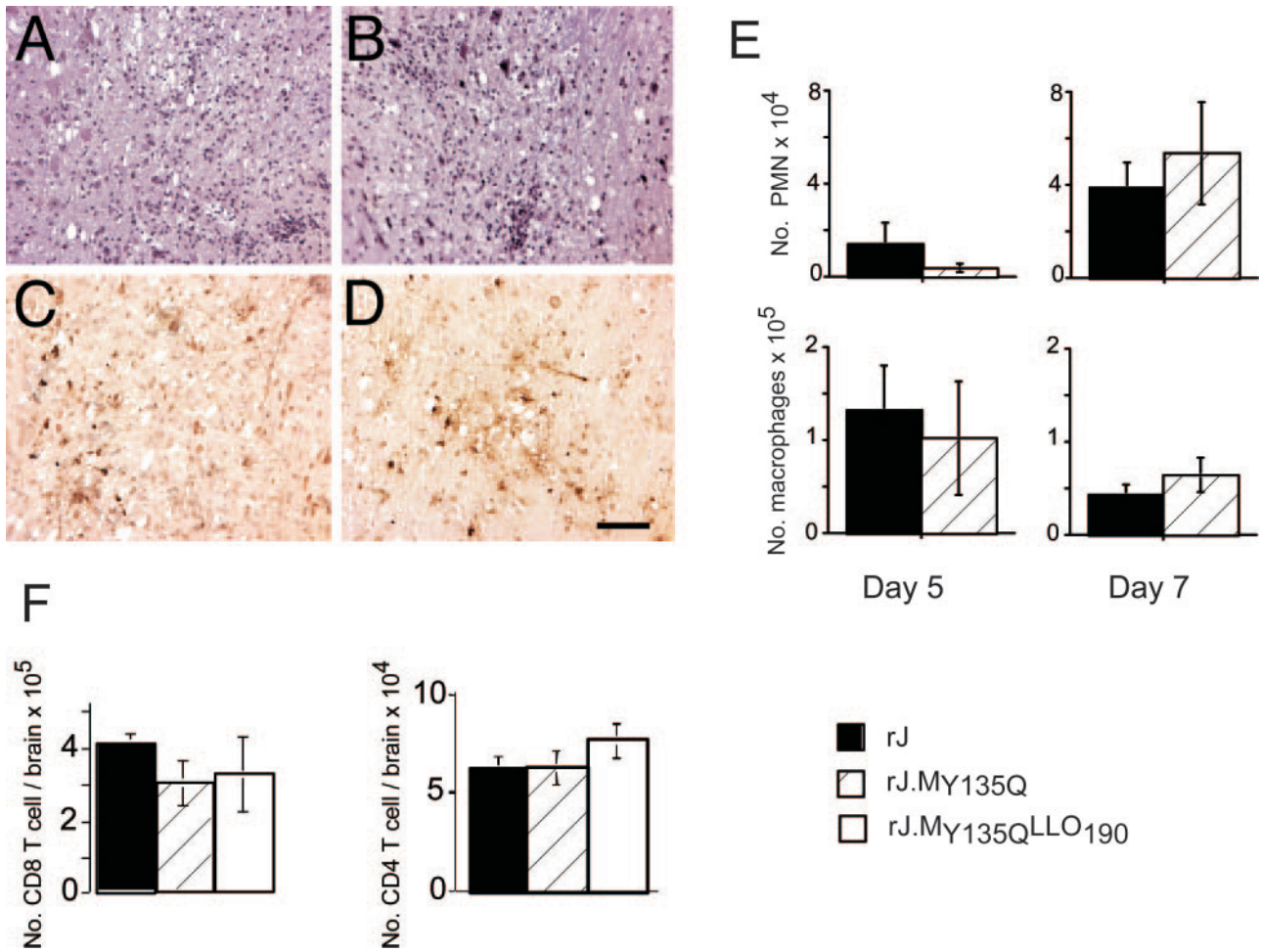


**Figure 5.** Inflammation and virus antigen in the CNS of mice infected with rJ or rJ.MY135Q. Brains were harvested from rJ- or rJ.MY135Q-infected mice and fixed in zinc formalin. Sagittal sections were prepared and stained with hematoxylin and eosin (**A** and **B**) or for virus antigen (**C** and **D**) as described in Materials and Methods. **A–D:** Photomicrographs of the dorsal midbrain. Similar numbers of infiltrating parenchymal and perivascular cells and of infected cells were detected in the CNS of mice infected with rJ (**A** and **C**) or rJ.MY135Q (**B** and **D**). Scale bar = 50  $\mu$ m. **E:** Numbers of neutrophils (CD45<sup>hi</sup>F4/80<sup>-</sup>Ly6G<sup>+</sup>) and macrophages/microglia (CD45<sup>int/hi</sup>F4/80<sup>+</sup>Ly6G<sup>-</sup>, “macrophages”) were determined as described in Materials and Methods. Seven rJ- and eight rJ.MY135Q-infected mice were analyzed in these assays. **F:** Total numbers of CD8 and CD4 T cells in the infected CNS were assayed as described in Materials and Methods. Seven and 15 rJ-, 7 and 19 rJ.MY135Q-, and 4 and 11 rJ.MY135Q.LLO190-infected mice were analyzed for CD8 T cells and CD4 T cells, respectively.

LLO190 substituted for the response to epitope M133 in mediating severe clinical disease.

#### Clinical Disease Was Equivalent in BALB/c Mice Infected with rJ.MY135Q or rJ.MY135Q.LLO190

To further confirm an important role for the CD4 T-cell response in the observed differences in disease outcome, we infected BALB/c mice with the three different viruses (Figure 6, A and B). The CD4 T-cell response in BALB/c mice (H-2<sup>d</sup> haplotype) is primarily directed at epitopes located within the nucleocapsid (N) and S proteins,<sup>37,38</sup> and epitopes LLO190 and M133 are not recognized in this strain of mice. The absence of epitope M133 should not result in an attenuated infection when BALB/c mice are infected with rJ.MY135Q, and consequently, rJ-, rJ.MY135Q-, and rJ.MY135Q.LLO190-infected BALB/c mice should develop encephalitis of equivalent severity. Infection with rJ.MY135Q or rJ.MY135Q.LLO190

caused similar mortality and weight loss in BALB/c mice, although mortality was less than in rJ-infected animals. Thus, these results showed that the presence of epitope LLO190 did not change the outcome in mice in which this epitope was not recognized. The lower mortality observed in rJ.MY135Q- or rJ.MY135Q.LLO190-infected mice, when compared with mice infected with rJ, suggested that rJ.MY135Q and rJ.MY135Q.LLO190 were slightly attenuated. As another approach to measuring virus attenuation, we infected RAG1<sup>-/-</sup> mice with rJ, rJ.MY135Q or rJ.MY135Q.LLO190 (Figure 6E). In the absence of an adaptive immune response, all three viruses caused lethal acute encephalitis with similar kinetics, suggesting that any attenuation caused by the MY135Q mutation was modest. Regardless, this attenuation, which may be related to the modest changes in thermostability conferred by the MY135Q mutation (Figure 3B), did not mask the pathogenic effect of epitope LLO190-specific CD4 T cells in rJ.MY135Q.LLO190-infected B6 mice (Figure 4, A and B).

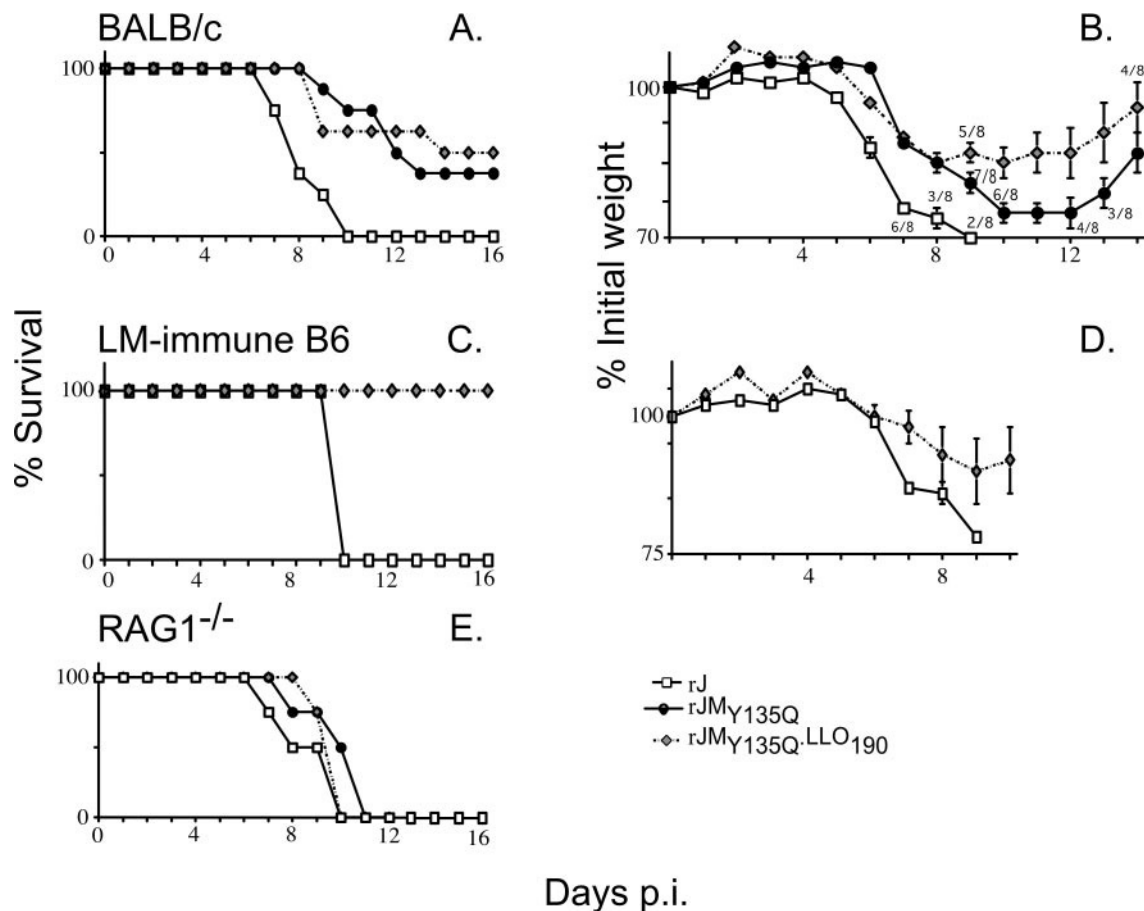


**Figure 6.** Mortality and weight loss in BALB/c, LM-immune, and *RAG1*<sup>-/-</sup> mice infected with recombinant viruses. Mice were infected with rJ, rJ.M<sub>Y135Q</sub>, or rJ.M<sub>Y135Q</sub>.LLO<sub>190</sub> and monitored for mortality (A, C, and E) and weight loss (B and D). In B and D, weight relative to weight at onset of experiment is shown for mice surviving at each time point. A and B: Eight BALB/c mice each were infected with rJ, rJ.M<sub>Y135Q</sub>, or rJ.M<sub>Y135Q</sub>.LLO<sub>190</sub> and monitored for survival and weight loss. C and D: Eight 5-week-old B6 mice were inoculated intraperitoneally with LM as described in Materials and Methods. Twenty-eight days later, four mice each were inoculated intranasally with either rJ or rJ.M<sub>Y135Q</sub>.LLO<sub>190</sub> and monitored for survival and weight loss. Data are representative of three independent experiments. E: rJ-, rJ.M<sub>Y135Q</sub>-, and rJ.M<sub>Y135Q</sub>.LLO<sub>190</sub>-infected *RAG1*<sup>-/-</sup> mice (*n* = 4 for each virus) were monitored for mortality. Data are representative of two independent experiments.

*Responses to Subdominant CD4 T-Cell Epitopes and to CD8 T-Cell Epitope S510 Were Similar in Mice Infected with rJ, rJ.M<sub>Y135Q</sub>, or rJ.M<sub>Y135Q</sub>.LLO<sub>190</sub>*

One explanation for our results is that more severe disease in rJ- and rJ.M<sub>Y135Q</sub>.LLO<sub>190</sub>-infected B6 mice reflected the presence of a greater number of virus-specific CD4 T cells in the CNS compared with those infected with rJ.M<sub>Y135Q</sub>. If valid, there should not be a compensatory increase in numbers of CD4 T cells responding to subdominant epitopes in rJ.M<sub>Y135Q</sub>-infected compared with rJ- or rJ.M<sub>Y135Q</sub>.LLO<sub>190</sub>-infected mice. At least two subdominant CD4 T-cell epitopes, located in the S protein (encompassing residues 333 to 347 and 358 to 372; epitope S333 and S358), are recognized in JHMV-infected B6 mice.<sup>14</sup> To determine whether the absence of the epitope M133-specific CD4 T-cell response changed the magnitude of the CD4 T-cell responses to these two epitopes, lymphocytes harvested from the CNS of mice infected with rJ, rJ.M<sub>Y135Q</sub>, and rJ.M<sub>Y135Q</sub>.LLO<sub>190</sub> were analyzed in intracellular cytokine assays. As shown in

Figure 7A and Table 2, we detected equivalent or diminished responses to epitopes S333 and S358 in rJ.M<sub>Y135Q</sub> or rJ.M<sub>Y135Q</sub>.LLO<sub>190</sub> mice compared with rJ-infected mice, showing that a compensatory increase in the CD4 T-cell response to these subdominant epitopes did not occur. We also compared the total number of CD4 T cells responding to known JHMV-specific CD4 T-cell epitopes. Not surprisingly, given the lack of compensatory increase in numbers of epitope S333- and epitope S358-specific CD4 T cells in rJ.M<sub>Y135Q</sub>-infected mice, the number of virus-specific CD4 T cells was significantly lower in rJ.M<sub>Y135Q</sub>-infected mice when compared with mice infected with rJ or rJ.M<sub>Y135Q</sub>.LLO<sub>190</sub> (Figure 7B) (*P* < 0.0001 and *P* = 0.011, respectively).

CD4 T cells are required for survival and optimal effector function of CD8 T cells in the JHMV-infected CNS.<sup>39</sup> Next, we determined whether there is a change in the number or function of virus-specific CD8 T cells in the absence of a response to epitope M133. The number of CNS-derived CD8 T cells responding to epitope S510 (the immunodominant epitope recognized in B6 mice, encompassing residues 510 to 518 of the S glycoprotein)

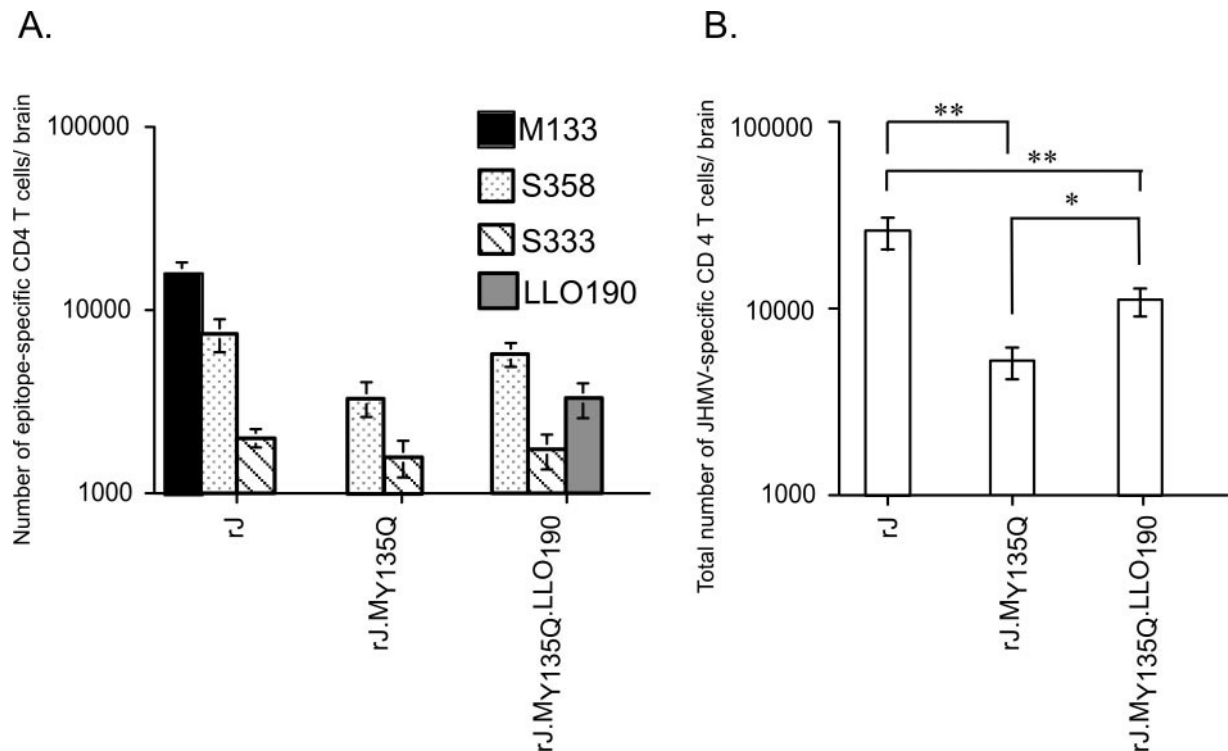


**Figure 7.** Response to subdominant JHMV-specific CD4 T-cell epitopes in the CNS of infected mice. Lymphocytes were harvested from the brains of 5- to 6-week-old B6 mice 7 days after infection with rJ, rJ.MY135Q, or rJ.MY135Q.LLO190. JHMV-specific CD4 T cells were identified by intracellular staining for IFN- $\gamma$ . Individual mice were analyzed in these assays. Eight to 12 mice infected with each virus were analyzed in two to three independent experiments. **A:** Numbers of cells responding to individual epitopes are shown. **B:** The number of total virus-specific CD4 T cells in each mouse was calculated by summing the number of cells responding to the individual epitopes indicated in **A**. The total number of virus-specific CD4 T cells in the CNS was significantly less in mice infected with rJ.MY135Q than in the CNS of mice infected with rJ or rJ.MY135Q.LLO190 (\*\* $P < 0.0001$ , \* $P = 0.011$ ).

tein<sup>27,40</sup>) was determined by staining with MHC class I/S510 tetramers. Equivalent numbers of epitope S510-specific CD8 T cells were detected in the CNS of mice infected with rJ or rJ.MY135Q (Figure 8A). To assess the effector function of these cells, we measured cytokine production and cytolytic activity directly *ex vivo*. After peptide S510 stimulation and intracellular IFN- $\gamma$  staining, we detected similar numbers of epitope-specific CD8 T cells in the CNS of mice infected with rJ, rJ.MY135Q, or rJ.MY135Q.LLO190 (Figure 8B; Table 2). Furthermore, equivalent fractions of epitope S510-specific CD8 T cells in the CNS of rJ- or rJ.MY135Q-infected mice, as identified by IFN- $\gamma$  staining, also expressed TNF- $\alpha$  (Figure 8C). Additionally, CD8 T cells isolated from rJ- or rJ.MY135Q-infected mice all exhibited similar levels of cytolytic activity against peptide S510-coated targets in direct *ex vivo* assays (Figure 8, D and E). In these assays, cytolytic activity was normalized to a per cell basis using D<sup>b</sup>/S510 tetramer staining.

### Virus-Specific Memory CD4 T Cells Are Protective and Do Not Cause Immunopathology

These results, which suggested that the CD4 T-cell response to epitope M133 in rJ-infected mice contributed to severe disease, contrast with a published report showing that adoptive transfer of a JHMV-specific CD4 T-cell clone was protective if cells were transferred before or 1 day after infection.<sup>41</sup> To resolve this apparent contradiction, we immunized B6 mice with an attenuated strain of LM. This strain of LM is cleared by 7 days after inoculation<sup>42</sup>. The number of CD4 T cells responding to LLO190 is greatly increased in LM-immune mice compared with naïve mice, because 3 to 4% of splenic CD4 T cells respond to the epitope at the peak of primary LM infection.<sup>43</sup> Consequently, LM-immune mice are expected to mount a robust CD4 T-cell response to epitope LLO190, expressed by rJ.MY135Q.LLO190 but not by rJ. Four weeks

**Table 2.** Antigen Specificity of CD8 T Lymphocytes Harvested from CNS of Mice at Day 7 p.i.

Virus	No. of Mice	% CD8	% S510 <sup>a</sup>	No. of S510 ( $\times 10^5$ ) <sup>*</sup>
rJ	4	24.3 $\pm$ 2.3	26.1 $\pm$ 2.3	1.5 $\pm$ 0.4
rJ.MY135Q	4	14.6 $\pm$ 1.9	34.2 $\pm$ 3.7	1.3 $\pm$ 0.5
rJ.MY135Q.LLO190	4	13.6 $\pm$ 3.4	30.2 $\pm$ 0.9	0.95 $\pm$ 0.3

<sup>a</sup>No. and percentage of CD8 T cells expressing IFN- $\gamma$  after *ex vivo* stimulation with peptide S510 after subtracting background (response to irrelevant peptide Ova 257–264).

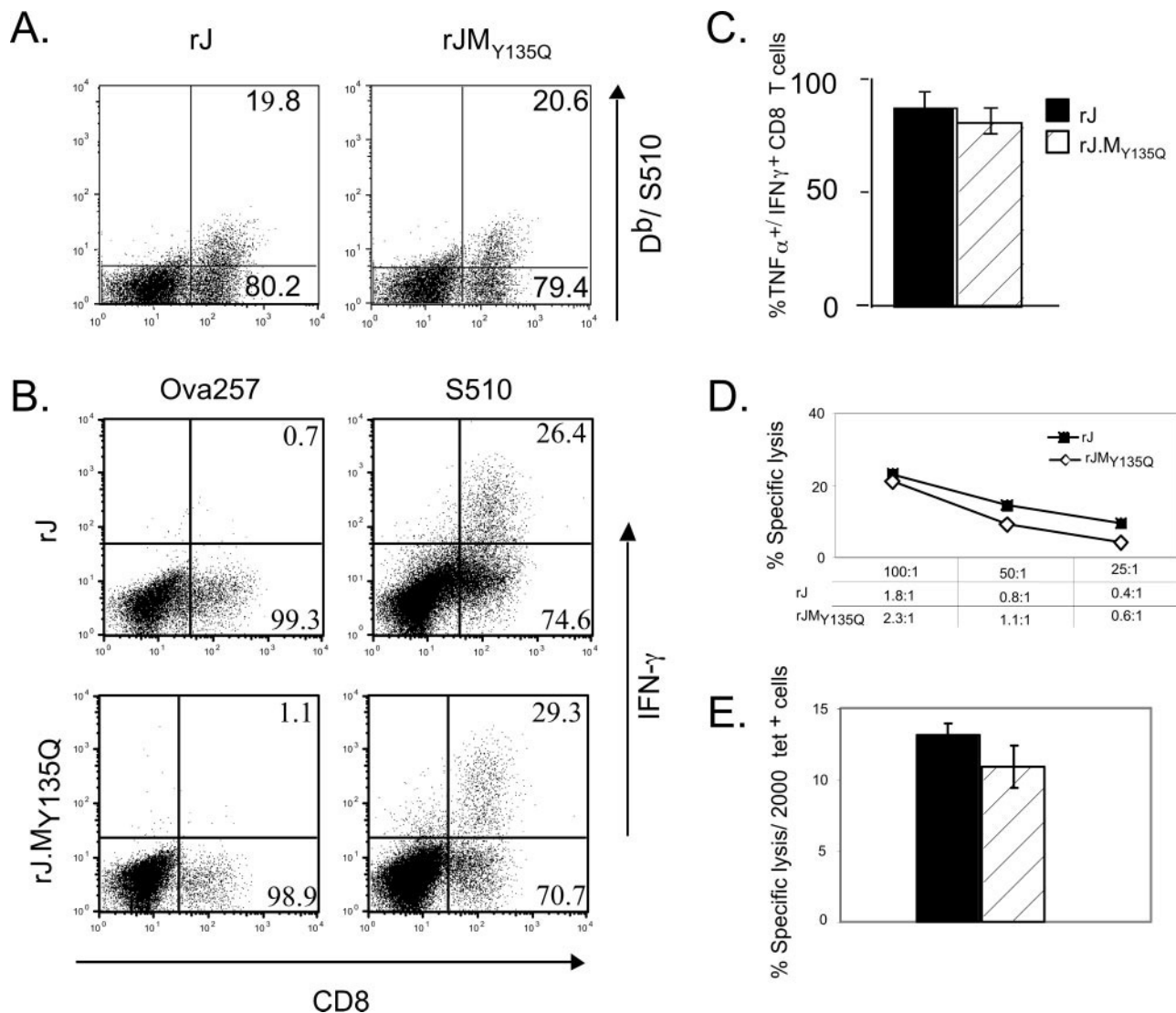


**Figure 8.** Virus-specific CD8 T-cell numbers and activity in the JHMV-infected CNS. Mononuclear cells were harvested from the brains of 5- to 6-week-old B6 mice 7 days p.i. as described in Materials and Methods. **A:** Cells were stained for surface CD8 and with D<sup>b</sup>/S510 tetramer S510. The percentage of tetramer<sup>+</sup> and tetramer<sup>-</sup> CD8 T cells is shown. **B:** JHMV-specific CD8 T cells were identified by intracellular staining for IFN-γ after stimulation with peptide S510 and FACS analysis. Individual mice were analyzed in these assays. The percentage of IFN-γ<sup>+</sup> and IFN-γ<sup>-</sup> CD8 T cells is shown. **C:** Four B6 mice were infected with rJ or rJ.M<sub>γ135Q</sub>. Cells were prepared from the CNS at day 7 p.i. and analyzed for TNF-α and IFN-γ expression after stimulation with peptide S510 as described in Materials and Methods. The results are expressed as the percentage of TNF-α<sup>+</sup>/IFN-γ<sup>+</sup> CD4 T cells. None of the differences between samples were statistically significant. **D** and **E:** CNS-derived mononuclear cells were prepared from mice infected with rJ (*n* = 3) or rJ.M<sub>γ135Q</sub> (*n* = 3) at 7 days p.i. *Ex vivo* cytolytic activity was assayed at the indicated E:T ratios using EL-4 target cells coated with 1 μmol/L peptide S510 or irrelevant peptide. Background cytolysis was < 8% in this experiment and was subtracted from specific release of peptide-coated targets. E:T ratios are displayed as either total populations or percentage of epitope S510-specific cells as determined by D<sup>b</sup>/S510 tetramer staining. Average cytolysis/2000 tetramers is shown in **E**. None of the differences between samples were statistically significant. Data are representative of three independent experiments.

after immunization with LM, mice were infected with rJ or rJ.M<sub>γ135Q</sub>.LLO<sub>190</sub>. As shown in Figure 6, C and D, the presence of LLO190-specific memory CD4 T cells protected mice from infection with rJ.M<sub>γ135Q</sub>.LLO<sub>190</sub> but not rJ. Mice infected with rJ.M<sub>γ135Q</sub>.LLO<sub>190</sub> exhibited some weight loss (Figure 6D) but developed only minor clinical signs of disease. The slight prolongation in survival time observed in rJ-infected LM-immune mice compared with rJ-infected naïve B6 mice likely occurred because mice were inoculated with virus at 9 weeks of age (28 days after infection with LM) in this experiment. By contrast, in the experiments described above, mice were infected when they were 5 to 6 weeks old. In summary, these

results show that virus-specific memory CD4 T cells, unlike naïve T cells, are protective in mice with acute encephalitis and do not mediate enhanced disease.

*Differences in Outcomes between Mice Infected with rJ or rJ.M<sub>γ135Q</sub>.LLO<sub>190</sub> and rJ.M<sub>γ135Q</sub> Are Not Due to Differential Th1/Th2-Type Responses or to Differences in TNF-α Expression*

Our results thus far are consistent with disease in mice infected with rJ or rJ.M<sub>γ135Q</sub>.LLO<sub>190</sub> but not rJ.M<sub>γ135Q</sub>,

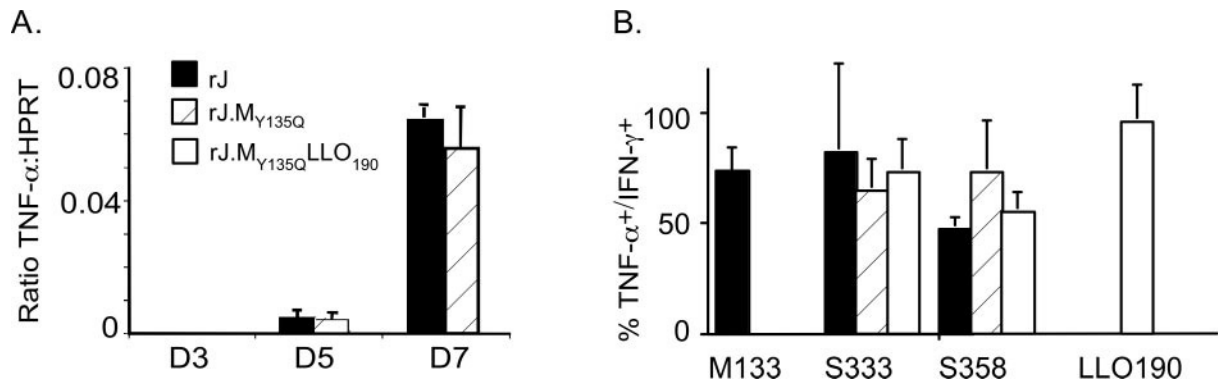


**Figure 9.** TNF- $\alpha$  expression in the infected CNS. **A:** RNA was harvested from the brains of mice infected with rJ ( $n = 3$ ) or rJ.M<sub>Y135Q</sub> ( $n = 3$ ) at each time point. The amount of TNF- $\alpha$  mRNA was quantified by real-time RT-PCR as described in Materials and Methods. **B:** Five B6 mice were infected with rJ, rJ.M<sub>Y135Q</sub>, or rJ.M<sub>Y135Q</sub>.LLO<sub>190</sub> and sacrificed at day 7 p.i. Cells were prepared from the CNS and analyzed for TNF- $\alpha$  and IFN- $\gamma$  expression after stimulation with the indicated peptides by intracellular cytokine staining as described in Materials and Methods. The results are expressed as the percentage of TNF- $\alpha$ <sup>+</sup>/IFN- $\gamma$ <sup>+</sup> CD4 T cells. None of the differences between samples were statistically significant.

reflecting quantitative differences in the numbers of anti-JHMV CD4 T cells in the CNS (Figure 7B). An alternative explanation is that anti-JHMV CD4 T cells in the CNS of rJ.M<sub>Y135Q</sub>-infected mice show a preferential Th2-type anti-inflammatory response. To examine this possibility, CNS-derived lymphocytes were prepared from B6 mice infected with rJ or rJ.M<sub>Y135Q</sub> at 7 days p.i. and analyzed for expression of two representative Th1/Th2 cytokines (IFN- $\gamma$  and IL-5). ELISPOT and intracellular cytokine assays were performed after stimulation with anti-CD3 and anti-CD28 mAb or with phorbol 12-myristate 13-acetate (PMA) (50 ng/ml) and ionomycin (500 ng/ml), respectively. Anti-CD3/anti-CD28 or PMA/ionomycin stimulation was used in these experiments to detect cytokine expression by all CD4 T cells in the infected CNS not just secretion by cells responding to known JHMV-specific CD4 T-cell epitopes. Most CNS-derived CD4 T cells expressed IFN- $\gamma$  after PMA/ionomycin stimulation when measured by intracellular cytokine assay (data not shown). No IL-5-secreting CD4 T cells could be detected by intracellular cytokine assay after stimulation with PMA/ionomycin, when four rJ-infected and five rJ.M<sub>Y135Q</sub>-infected mice were analyzed. However, using the more sensitive ELISPOT assay, we detected low but equivalent numbers of IL-5-secreting CD4 T cells in the CNS of mice infected with either rJ or rJ.M<sub>Y135Q</sub> (rJ: 19.2 of 10,000; range, 13.7 to 24.8; two mice) (rJ.M<sub>Y135Q</sub>: 20.9 of 10,000  $\pm$  6.9,  $n = 5$ ). Furthermore, each responding cell secreted approximately the same amount of IL-5 because spot size was equivalent in all samples. Thus, it is unlikely that change to a Th2-type response is responsible for the mild clinical disease observed in rJ.M<sub>Y135Q</sub>-infected mice.

Another possible explanation is that levels of TNF- $\alpha$ , a pleiotropic cytokine implicated in the development of sepsis-like syndromes in several human and experimental infections,<sup>44,45</sup> are decreased in rJ.M<sub>Y135Q</sub>-infected mice. TNF- $\alpha$  is produced largely by macrophages and glial cells in the JHMV-infected CNS,<sup>46</sup> but CD4 T cells also produce this cytokine after antigen contact.<sup>43</sup> To assess the role of TNF- $\alpha$ , RNA was harvested from the CNS of rJ- and rJ.M<sub>Y135Q</sub>-infected mice at 3, 5, and 7

days p.i. and analyzed by real-time RT-PCR. We detected similar levels of TNF- $\alpha$  mRNA in the CNS of mice infected with rJ or rJ.M<sub>Y135Q</sub> (Figure 9A). As a second approach, we determined whether there were differences in TNF- $\alpha$  expression by JHMV-specific CD4 T cells after stimulation with cognate antigen. Lymphocytes were harvested from the CNS of mice infected with rJ, rJ.M<sub>Y135Q</sub>, or rJ.M<sub>Y135Q</sub>.LLO<sub>190</sub> and analyzed for IFN- $\gamma$  and TNF- $\alpha$  production after stimulation with peptides corresponding to JMV-specific CD4 T-cell epitopes (epitopes M133, S329, S358, and LLO190). As shown in Figure 9B, similar proportions of each epitope-specific CD4 T-cell population, as defined by IFN- $\gamma$  expression, also elaborated TNF- $\alpha$ , independent of whether the cells were harvested from the rJ-, rJ.M<sub>Y135Q</sub>-, or rJ.M<sub>Y135Q</sub>.LLO<sub>190</sub>-infected CNS.

### Discussion

Herein, we show that genetic disruption of a single JHMV-specific CD4 T-cell epitope is beneficial to the host, greatly decreasing the morbidity and mortality observed in mice with murine coronavirus-induced encephalitis. Although the role of virus-specific CD4 T cells in JHMV-induced demyelination has been previously described,<sup>11,16</sup> our results show that CD4 T cells also have a major pathogenic role in the acute encephalitis mediated by JHMV. Abrogation of the response to the immunodominant M133 epitope resulted in amelioration of clinical disease, in the absence of any effect on the kinetics of virus clearance (Figure 4). The mutation in the M protein resulted in a small change in virus thermostability (Figure 3B), which may have contributed to the lower mortality that we detected in rJ.M<sub>Y135Q</sub>- or rJ.M<sub>Y135Q</sub>.LLO<sub>190</sub>-infected compared with rJ-infected BALB/c mice (Figure 6A). However, this change did not account for the lack of lethality observed in rJ.M<sub>Y135Q</sub>-infected B6 mice because the introduction of RNA encoding an exogenous CD4 T-cell epitope (LLO<sub>190</sub>) into the genome of rJ.M<sub>Y135Q</sub> resulted in restoration of severe disease. Furthermore, *RAG1*<sup>-/-</sup> mice died with similar kinetics when infected with rJ, rJ.M<sub>Y135Q</sub>, or rJ.M<sub>Y135Q</sub>.LLO<sub>190</sub>.

Our results might reflect quantitative or qualitative differences in anti-JHMV CD4 T cells. Precedent for qualitative differences in CD4 T cells comes from several studies. Mice chronically infected with another neurotropic virus, Theiler's murine encephalomyelitis virus (TMEV), develop a Th1-type CD4 T cell-mediated demyelinating disease, but disease is ameliorated when mice are infected with a variant TMEV that encodes a mutated CD4 T-cell epitope; infection with this variant results in a predominant Th2-type response and low pathogenicity.<sup>47</sup> In another example, mice immunized with vaccinia virus expressing the G protein (VV-G) of respiratory syncytial virus (RSV) and subsequently infected with wild-type RSV develop immune-mediated respiratory disease.<sup>48</sup> A single immunodominant RSV-specific CD4 T-cell epitope and no CD8 T-cell epitopes are present within the G protein, and immunization with VV-G induces an exaggerated Th2-type response to this epitope. In this case, unlike TMEV-infected mice, a Th2-type CD4 T-cell response is immunopathological. However, differential induction of Th1/Th2 responses is unlikely to explain our results because most cells in the CNS of mice infected with rJ or rJ.M<sub>Y135Q</sub> express IFN- $\gamma$ , and few express IL-5, a Th2-type cytokine. Our results are also not likely to be explained by intrinsic differences between the different JHMV-specific CD4 T-cell epitopes because epitope M133, present in rJ, and epitopes S333 and S358, present in both rJ and rJ.M<sub>Y135Q</sub>, exhibited similar functional avidity as measured in proliferation assays.<sup>14</sup>

At this juncture, we favor a quantitative explanation for our results. The number of virus-specific CD4 T cells was significantly lower in the CNS of rJ.M<sub>Y135Q</sub>-infected B6 mice than in mice infected with rJ or rJ.M<sub>Y135Q</sub>.LLO<sub>190</sub> (Figure 7B). Support for the notion that disease occurs when numbers of virus-specific CD4 T cells are elevated comes from a study of a variant of lymphocytic choriomeningitis virus (LCMV) that lacked one of two immunodominant CD4 T-cell epitopes.<sup>49</sup> Mice infected with variant but not wild-type LCMV mounted a robust anti-virus neutralizing antibody response and cleared virus more efficiently. More anti-LCMV neutralizing antibody was also produced in mice infected with wild-type LCMV if CD4 T cells were partially and transiently depleted with anti-CD4 antibody before infection. Our results, like those of Recher et al, show that a less robust CD4 T-cell response may result in less immunopathological disease without diminishing the kinetics of virus clearance. They support the notion that this is primarily a quantitative effect (Figure 7B).

How could a difference in numbers of JHMV-specific CD4 T cells affect morbidity and mortality? CD4 T cells are required for optimal CD8 T-cell effector function in the JHMV-infected CNS,<sup>39</sup> and it is possible that fewer numbers of fully active anti-JHMV CD8 T cells could result in diminished immunopathogenic disease. However, we detected similar numbers of epitope S510-specific CD8 T cells in the CNS of mice infected with rJ or rJ.M<sub>Y135Q</sub> when measured by tetramer staining, cytokine secretion, or cytolytic activity (Figure 8). An attractive possibility is that virus-specific CD4 T cells express one or more products that have pathogenic effects; these effects become apparent when the numbers of cells exceed a certain

level. We investigated TNF- $\alpha$  as a candidate molecule because TNF- $\alpha$  production by CD4 T cells, unlike CD8 T cells, does not cease after prolonged exposure to antigen<sup>43</sup> and T-cell expression of this cytokine correlates with pathogenicity in other virus infections. For example, TNF- $\alpha$  produced by virus-specific CD8 T cells is the principal mediator of clinical illness in mice infected with RSV; administration of anti-TNF- $\alpha$  antibody resulted in significantly attenuated illness with only slight effects on the kinetics of virus clearance.<sup>50</sup> However, we detected no differences in TNF- $\alpha$  mRNA levels in the brains of mice infected with rJ, rJ.M<sub>Y135Q</sub>, or rJ.M<sub>Y135Q</sub>.LLO<sub>190</sub> (Figure 9A) and no differences in the proportion of JHMV-specific CD4 T cells harvested from mice infected with rJ, rJ.M<sub>Y135Q</sub>, or rJ.M<sub>Y135Q</sub>.LLO<sub>190</sub> that secreted TNF- $\alpha$  after stimulation with JHMV-specific peptide (Figure 9B). Of note, TNF- $\alpha$  may still have localized effects at sites of CD4 T-cell accumulation. Because TNF- $\alpha$  is involved in the regulation of multiple functions in the CNS, including thermoregulation, appetite, and the development of seizures,<sup>51-54</sup> differential localized expression by CD4 T cells may directly effect the development of clinical signs or may trigger the expression of secondary pro-inflammatory mediators.

Our results may have implications for understanding the mechanism of encephalitis in general. An immunopathological component has been identified in several chronic human and animal CNS infections, including humans infected with HIV-1 and mice infected with JHMV or Theiler's encephalomyelitis virus.<sup>1,55</sup> However, the rapidly fatal outcomes observed in some patients with acute viral encephalitis are generally attributed to direct virus destruction of infected cells. Our results show that the T-cell response, in the setting of a large number of infected target cells, may also contribute to disease, even at relatively early times after infection. Consequently, our results suggest that modulation of the numbers of anti-virus CD4 T cells responding to a single epitope may attenuate disease without adversely affecting virus clearance.

## Acknowledgments

We thank Drs. John Harty and Steven Varga and members of the Perlman laboratory for critical review of the manuscript and Katherine O'Malley for technical assistance.

## References

1. Stohman SA, Hinton DR: Viral induced demyelination. *Brain Pathol* 2001, 11:92-106
2. Stohman SA, Bergmann CC, Perlman S: Mouse Hepatitis Virus. Edited by R Ahmed, I Chen. New York, John Wiley & Sons, Ltd., 1998, pp 537-557
3. Barnett E, Cassell M, Perlman S: Two neurotropic viruses, herpes simplex virus type I and mouse hepatitis virus, spread along different neural pathways from the main olfactory bulb. *Neuroscience* 1993, 157:1007-1025
4. Barnett E, Perlman S: The olfactory nerve and not the trigeminal nerve is the major site of CNS entry for mouse hepatitis virus, strain JHM. *Virology* 1993, 194:185-191
5. Perlman S, Evans G, Afifi A: Effect of olfactory bulb ablation on spread

- of a neurotropic coronavirus into the mouse brain. *J Exp Med* 1990, 172:1127–1132
6. Williamson JS, Sykes KC, Stohlman SA: Characterization of brain-infiltrating mononuclear cells during infection with mouse hepatitis virus strain JHM. *J Neuroimmunol* 1991, 32:199–207
  7. Haring JS, Pewe LL, Perlman S: High magnitude, virus-specific CD4 T-cell response in the central nervous system of coronavirus-infected mice. *J Virol* 2001, 75:3043–3047
  8. Rempel JD, Murray SJ, Meisner J, Buchmeier MJ: Differential regulation of innate and adaptive immune responses in viral encephalitis. *Virology* 2004, 318:381–392
  9. Weiner LP: Pathogenesis of demyelination induced by a mouse hepatitis virus (JHM virus). *Arch Neurol* 1973, 28:298–303
  10. Williamson JS, Stohlman SA: Effective clearance of mouse hepatitis virus from the central nervous system requires both CD4<sup>+</sup> and CD8<sup>+</sup> T cells. *J Virol* 1990, 64:4589–4592
  11. Pewe L, Haring J, Perlman S: CD4 T-cell-mediated demyelination is increased in the absence of gamma interferon in mice infected with mouse hepatitis virus. *J Virol* 2002, 76:7329–7333
  12. Wu GF, Dandekar AA, Pewe L, Perlman S: CD4 and CD8 T cells have redundant but not identical roles in virus-induced demyelination. *J Immunol* 2000, 165:2278–2286
  13. Wu GF, Perlman S: Macrophage infiltration, but not apoptosis, is correlated with immune-mediated demyelination following murine infection with a neurotropic coronavirus. *J Virol* 1999, 73:8771–8780
  14. Xue S, Perlman S: Antigen specificity of CD4 T cell response in the central nervous system of mice infected with mouse hepatitis virus. *Virology* 1997, 238:68–78
  15. Njenga MK, Pavelko K, Baisch J, Lin X, David C, Leibowitz JL, Rodriguez M: Theiler's virus persistence and demyelination in major histocompatibility complex class II-deficient mice. *J Virol* 1996, 70:1729–1737
  16. Houtman JJ, Fleming JO: Dissociation of demyelination and viral clearance in congenitally immunodeficient mice infected with murine coronavirus JHM. *J Neurovirol* 1996, 2:101–110
  17. Liu T, Chambers TJ: Yellow fever virus encephalitis: properties of the brain-associated T-cell response during virus clearance in normal and gamma interferon-deficient mice and requirement for CD4<sup>+</sup> lymphocytes. *J Virol* 2001, 75:2107–2118
  18. Murali-Krishna K, Ravi V, Manjunath R: Protection of adult but not newborn mice against lethal intracerebral challenge with Japanese encephalitis virus by adoptively transferred virus-specific cytotoxic T lymphocytes: requirement for L3T4<sup>+</sup> T cells. *J Gen Virol* 1996, 77:705–714
  19. Weidinger G, Henning G, ter Meulen V, Niewiesk S: Inhibition of major histocompatibility complex class II-dependent antigen presentation by neutralization of gamma interferon leads to breakdown of resistance against measles virus-induced encephalitis. *J Virol* 2001, 75:3059–3065
  20. Perlman S, Schelper R, Bolger E, Ries D: Late onset, symptomatic, demyelinating encephalomyelitis in mice infected with MHV-JHM in the presence of maternal antibody. *Microb Pathog* 1987, 2:185–194
  21. Ontiveros E, Kuo L, Masters PS, Perlman S: Inactivation of expression of gene 4 of mouse hepatitis virus strain JHM does not affect virulence in the murine CNS. *Virology* 2001, 290:230–238
  22. Kuo L, Godeke GJ, Raamsman MJ, Masters PS, Rottier PJ: Retargeting of coronavirus by substitution of the spike glycoprotein ectodomain: crossing the host cell species barrier. *J Virol* 2000, 74:1393–1406
  23. Geginat G, Schenk S, Skoberne M, Goebel W, Hof H: A novel approach of direct ex vivo epitope mapping identifies dominant and subdominant CD4 and CD8 T cell epitopes from *Listeria monocytogenes*. *J Immunol* 2001, 166:1877–1884
  24. Pewe L, Wu G, Barnett EM, Castro R, Perlman S: Cytotoxic T cell-resistant variants are selected in a virus-induced demyelinating disease. *Immunity* 1996, 5:253–262
  25. Krueger DK, Kelly SM, Lewicki DN, Ruffolo R, Gallagher TM: Variations in disparate regions of the murine coronavirus spike protein impact the initiation of membrane fusion. *J Virol* 2001, 75:2792–2802
  26. Pewe L, Heard SB, Bergmann CC, Dailey MO, Perlman S: Selection of CTL escape mutants in mice infected with a neurotropic coronavirus: quantitative estimate of TCR diversity in the infected CNS. *J Immunol* 1999, 163:6106–6113
  27. Castro RF, Perlman S: CD8<sup>+</sup> T cell epitopes within the surface glycoprotein of a neurotropic coronavirus and correlation with pathogenicity. *J Virol* 1995, 69:8127–8131
  28. Varga SM, Wissinger EL, Braciale TJ: The attachment (G) glycoprotein of respiratory syncytial virus contains a single immunodominant epitope that elicits both Th1 and Th2 CD4<sup>+</sup> T cell responses. *J Immunol* 2000, 165:6487–6495
  29. Pewe L, Zhou H, Netland J, Tangadu C, Olivares H, Shi L, Look D, Gallagher TM, Perlman S: A severe acute respiratory syndrome-associated coronavirus-specific protein enhances virulence of an attenuated murine coronavirus. *J Virol* 2005, 79:11335–11342
  30. Masters PS: Reverse genetics of the largest RNA viruses. *Adv Virus Res* 1999, 53:245–264
  31. Yount B, Denison MR, Weiss SR, Baric RS: Systematic assembly of a full-length infectious cDNA of mouse hepatitis virus strain A59. *J Virol* 2002, 76:11065–11078
  32. Wall KA, Hu J-Y, Currier P, Southwood S, Sette A, Infante A: A disease-related epitope of Torpedo acetylcholine receptor: residues involved in I-A<sup>b</sup> binding, self-nonself discrimination, and TCR antagonism. *J Immunol* 1994, 152:4526–4536
  33. Vennema H, Godeke G-J, Rossen JWA, Voorhout WF, Horzinek MC, Opstelten D-JE, Rottier PJM: Nucleocapsid-independent assembly of coronavirus-like particles by co-expression of viral envelope protein genes. *EMBO J* 1996, 15:2020–2028
  34. Ontiveros E, Kim TS, Gallagher TM, Perlman S: Enhanced virulence mediated by the murine coronavirus, mouse hepatitis virus strain JHM, is associated with a glycine at residue 310 of the spike glycoprotein. *J Virol* 2003, 77:10260–10269
  35. Lane TE, Liu MT, Chen BP, Asensio VC, Samawi RM, Paoletti AD, Campbell IL, Kunkel SL, Fox HS, Buchmeier MJ: A central role for CD4<sup>+</sup> T-cells and RANTES in virus-induced central nervous system inflammation and demyelination. *J Virol* 2000, 74:1415–1424
  36. Tran EH, Prince EN, Owens T: IFN-gamma shapes immune invasion of the central nervous system via regulation of chemokines. *J Immunol* 2000, 164:2759–2768
  37. Van der Veen RC: Immunogenicity of JHM virus proteins: characterization of a CD4<sup>+</sup> T cell epitope on nucleocapsid protein which induces different T-helper cell subsets. *Virology* 1996, 225:339–346
  38. Heemskerck M, Schoemaker H, De Jong I, Schijns V, Spaan W, Boog CJ: Differential activation of mouse hepatitis virus-specific CD4<sup>+</sup> cytotoxic T cells is defined by peptide length. *Immunology* 1995, 85:517–522
  39. Stohlman SA, Bergmann CC, Lin MT, Cua DJ, Hinton DR: CTL effector function within the central nervous system requires CD4<sup>+</sup> T cells. *J Immunol* 1998, 160:2896–2904
  40. Bergmann CC, Yao Q, Lin M, Stohlman SA: The JHM strain of mouse hepatitis virus induces a spike protein-specific D<sup>b</sup>-restricted CTL response. *J Gen Virol* 1996, 77:315–325
  41. Yamaguchi K, Goto N, Kyuwa S, Hayami M, Toyoda Y: Protection of mice from a lethal coronavirus infection in the central nervous system by adoptive transfer of virus-specific T cell clones. *J Neuroimmunol* 1991, 32:1–9
  42. Badovinac VP, Porter BB, Harty JT: CD8<sup>+</sup> T cell contraction is controlled by early inflammation. *Nat Immunol* 2004, 5:809–817
  43. Corbin GA, Harty JT: T cells undergo rapid ON/OFF but not ON/OFF/ON cycling of cytokine production in response to antigen. *J Immunol* 2005, 174:718–726
  44. Dinarello CA: Cytokines as mediators in the pathogenesis of septic shock. *Curr Top Microbiol Immunol* 1996, 216:133–165
  45. Beutler B, Cerami A: The biology of cachectin/TNF- $\alpha$  primary mediator of the host response. *Annu Rev Immunol* 1989, 7:625–655
  46. Haring JS, Pewe LL, Perlman S: Bystander CD8 T cell-mediated demyelination after viral infection of the central nervous system. *J Immunol* 2002, 169:1550–1555
  47. Palma JP, Yauch RL, Kang HK, Lee HG, Kim BS: Preferential induction of IL-10 in APC correlates with a switch from Th1 to Th2 response following infection with a low pathogenic variant of Theiler's virus. *J Immunol* 2002, 168:4221–4230
  48. Varga SM, Wang X, Welsh RM, Braciale TJ: Immunopathology in RSV infection is mediated by a discrete oligoclonal subset of antigen-specific CD4(+) T cells. *Immunity* 2001, 15:637–646
  49. Recher M, Lang KS, Hunziker L, Freigang S, Eschli B, Harris NL, Navarini A, Senn BM, Fink K, Lotscher M, Hangartner L, Zellweger R, Hersberger M, Theodorides A, Hangartner H, Zinkernagel RM: De-

- liberate removal of T cell help improves virus-neutralizing antibody production. *Nat Immunol* 2004, 5:934–942.
50. Rutigliano JA, Graham BS: Prolonged production of TNF-alpha exacerbates illness during respiratory syncytial virus infection. *J Immunol* 2004, 173:3408–3417
  51. Hehlgans T, Pfeffer K: The intriguing biology of the tumour necrosis factor/tumour necrosis factor receptor superfamily: players, rules and the games. *Immunology* 2005, 115:1–20
  52. Balosso S, Ravizza T, Perego C, Peschon J, Campbell IL, De Simoni MG, Vezzani A: Tumor necrosis factor-alpha inhibits seizures in mice via p75 receptors. *Ann Neurol* 2005, 57:804–812
  53. Conti B, Tabarean I, Andrei C, Bartfai T: Cytokines and fever. *Front Biosci* 2004, 9:1433–1449
  54. Marchetti L, Klein M, Schlett K, Pfizenmaier K, Eisel UL: Tumor necrosis factor (TNF)-mediated neuroprotection against glutamate-induced excitotoxicity is enhanced by N-methyl-D-aspartate receptor activation: essential role of a TNF receptor 2-mediated phosphatidylinositol 3-kinase-dependent NF-kappa B pathway. *J Biol Chem* 2004, 279:32869–32881
  55. Kaul M, Garden GA, Lipton SA: Pathways to neuronal injury and apoptosis in HIV-associated dementia. *Nature* 2001, 410:988–994